Earth and Planetary Science Letters 619 (2023) 118314

Contents lists available at ScienceDirect

Earth and Planetary Science Letters

journal homepage: www.elsevier.com/locate/epsl

Tertiary creep behavior for various rate- and state-dependent friction laws

Hiroyuki Noda[a,*], Chengrui Chang[b]

[a] Disaster Prevention Research Institute, Kyoto University, Gokasho, Uji, 6110011, Japan
[b] Graduate School of Agricultural and Life Sciences, the University of Tokyo, 1-1-1, Yayoi, Bunkyo-ku, Tokyo, 1138657, Japan

ARTICLE INFO

Article history:
Received 13 December 2022
Received in revised form 22 June 2023
Accepted 10 July 2023
Available online 3 August 2023
Editor: J.P. Avouac

Keywords:
rate- and state-dependent friction
creep test
landslides
failure-time forecast

ABSTRACT

Forecasting the acceleration of slow landslides to the point of catastrophic failure is crucial. It follows the Voight power-law model with the power exponent α, which is typically close to 2 but can be significantly smaller. Understanding the underlying mechanisms may improve landslide warnings. A previous study applied a rate- and state-dependent friction (RSF) law in the form of the aging law to the creep behavior of an underlying shear zone of landslides, and showed an α value of 2. The aging law is one of the conventional forms of RSF law, and we extended the analysis to other representative laws: the slip law, Perrin-Rice-Zheng (PRZ) law, composite law, and Nagata law. We showed that the acceleration is expressed in terms of the slip rate using the state-evolution equation. As the slip rate increases, α decays to 2, regardless of the frictional parameters, following a power law for the aging and Nagata laws and logarithmically for the slip and the composite laws. For the PRZ law, the asymptotic value of α is between 2 and 3 and depends on frictional parameters. In typical RSF laws, the logarithm of the slip rate is proportional to the friction coefficient or normalized shear stress f minus frictional strength Θ. The logarithmic direct effect and a linear increase with slip in $f - \Theta$ independent of the slip rate, which is a characteristic of aging and Nagata laws under constant stress conditions, leads to $\alpha = 2$. By contrast, a purely time-dependent increase in $f - \Theta$ would lead to $\alpha = 1$. If these two effects coexist, α increases from 1 to 2 with acceleration. In laboratory experiments of investigation of RSF law, constant-load creep tests in the tertiary-creep stage have been rarely conducted, but they could provide new insights on the form of the state-evolution equation and deserve future study.

1. Introduction

Slow landslides can accelerate to catastrophic failure (e.g., Lacroix et al., 2020) and cause disasters [e.g., 1963 Vaiont landslide (Müller, 1964; Hendron and Patton, 1985), 1983 Sale Mountain landslide (Zhang et al., 2002), 2012 Preonzo landslide (Loew et al., 2017), and 2017 Maoxian landslide (Intrieri et al., 2018)]. Prediction of future behavior of a slow landslide is crucial. Fukuzono (1985) proposed an empirical power-law relationship based on meters-scale slope-failure experiments between deformation rate $\dot{\Omega}$ and its acceleration $\ddot{\Omega}$,

$$\ddot{\Omega} = A\dot{\Omega}^{\alpha}, \tag{1}$$

where the dot represents the derivative with respect to time t, Ω is the measurable deformation such as surface displacement or opening of surface fractures, and A and α are empirical parameters. This law was subsequently applied to other phenomena such as volcanic eruptions (Voight, 1988) and failures in experiments for rate-dependent material (Voight, 1989), and is now referred to as the Voight model of failure-time forecast (Federico et al., 2012; Intrieri et al., 2019). The values of α for many landslides were estimated. Segalini et al. (2018) analyzed 26 cases and reported α from 1.53 to 2.15 with only 3 cases with $\alpha < 1.9$. Intrieri et al. (2019) reported a greater variation including cases with $\alpha < 1$. Bozzano et al. (2014) analyzed landslides involving cut slopes with and without artificial reinforcement, and obtained a minimum α of 0.62. In addition, α can differ for various acceleration events in the same location (e.g., Crosta and Agliardi, 2003). It is likely that α depends on the material and mechanism dominating the acceleration, and its understanding may lead to improved landslide warnings.

In laboratory constant-load creep tests (hereafter just “creep test”) for soil (e.g., Saito and Uezawa, 1961), the strain rate firstly

* Corresponding author.
E-mail addresses: noda.hiroyuki.7z@kyoto-u.ac.jp (H. Noda), chang-chengrui@g.ecc.u-tokyo.ac.jp (C. Chang).

https://doi.org/10.1016/j.epsl.2023.118314

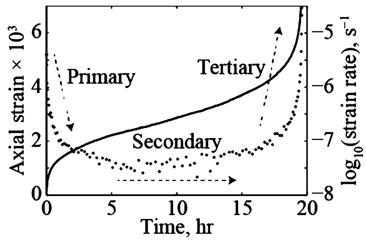

Fig. 1. Typical creep experiment. Axial strain (a black line) and strain rate (dots) during a triaxial creep test for sandstone by Brantut et al. (2014), showing primary, secondary, and tertiary creep behaviors. Modified from Fig. 1 in Brantut et al. (2014).

decays to an approximately constant level, and then increases towards failure. The behaviors in the deceleration, constant, and acceleration stages are called the primary, secondary, and tertiary creep, respectively. Voight (1989) found $\alpha \approx 2$ for the tertiary creep in laboratory experiments for soils, as well as for alloys and metals. Triaxial creep tests for sandstone (e.g., Yang and Jiang, 2010; Brantut et al., 2014) also shows the tertiary creep behavior. Fig. 1 is an example experimental data (Brantut et al., 2014), showing the three-stages behavior during a creep test. In the brittle regime, the tertiary creep behavior is typically associated with localization of deformation or faulting.

Measured surface deformation in the field involves non-localized deformation within the landslide mass and the localized slip beneath. In the initial stage of a landslide, the through-going slip surface may not have developed, and Ω may be dominated by the former. Slip propagation beneath the landslide mass has been observed prior to catastrophic failures (e.g., Cooper et al., 1998; Petley et al., 2002, 2005). After a through-going shear zone is developed, the surface deformation may be dominated by the slip, and the slip rate V can be regarded as the rate of measured deformation Ω in Eq. (1),

$$\dot{V} = AV^{\alpha}; \tag{2}$$

α is then expressed as

$$\alpha = \frac{V}{\dot{V}} \frac{\mathrm{d}\dot{V}}{\mathrm{d}V}. \tag{3}$$

Among many possible mechanisms, Helmstetter et al. (2004) analyzed acceleration of a frictional surface governed by a rate- and state-dependent friction (RSF) law in the form of the aging law (Dieterich, 1979; Ruina, 1983) under a constant stress state, revealing an $\alpha = 2$ regardless of the frictional parameters for a rate-weakening shear zone. It should be noted that the aging law is one of the most conventional RSF laws and many other laws have been published. The aim of this paper is to extend the study to different RSF laws and to observe the variability of α. In particular, if α depends on frictional parameters that can be measured in the laboratory, then we may be able to better determine the fate of slow landslides.

The RSF law can express not only the instantaneous relationship between the friction coefficient [shear stress / effective normal stress (Terzaghi, 1950)] f and the slip rate V, but also the evolution of the frictional strength (Dieterich, 1979). The instantaneous effect is often called the direct effect. The functional form of the RSF law, however, has been long debated and many different versions have been published for the evolution of the frictional strength. The aging law can reproduce laboratory-observed logarithmic time-dependent strengthening (Dieterich, 1972) in a limit of $V \to 0$ (log-t healing, Nakatani and Mochizuki, 1996), but yields non-symmetric decays of the friction coefficient f to its steady-state value f_{ss} after positive and negative steps of V (Marone, 1998). Another conventional law, the slip law, shows symmetric exponential decays of f to f_{ss} as a function of slip displacement that agree with laboratory experiments, it but lacks log-t healing (Beeler et al., 1994). Marone (1998) stated that the Perrin-Rice-Zheng (PRZ) law (Perrin et al., 1995) includes both log-t healing and symmetric decays but Nakatani (2001) has pointed out that the weakening from static friction is too rapid in the initial phase, compared with the laboratory result of exponential decay with slip. Subsequently, Kato and Tullis (2001) proposed a composite law by introducing a log-t healing term with a cut-off slip rate V_c into the slip law, but the composite law has a drawback that steady-state friction below V_c is significantly higher than observation. Nagata et al. (2012) formulated a state-evolution equation based on monitoring of the transmissibility of a high-frequency elastic wave across a sliding surface and improved the aging law to yield more symmetric decays but the asymmetry is still evident for larger velocity steps (Bhattacharya et al., 2015). These friction laws are studied here.

Note that more recently, Bhattacharya et al. (2017, 2022) showed that the slip law reproduces not only the velocity-step tests, but also typical slide-hold-slide (SHS) tests without controlling f during the hold period, arguing that the experimentally observed healing during the hold time is due to slow slip then caused by finite shear stress. On the other hand, Nakatani and Mochizuki (1996) showed the log-t healing by SHS tests with almost zero f during the hold period. In addition, the log-t healing is consistent with the time-dependent growth of real area of contact during stationary normal loading without shear stress directly observed by Dieterich and Kilgore (1994).

In the next section, we briefly explain the framework of the RSF law, the circumstances for acceleration to occur, and the expression of acceleration commonly applicable to different state-evolution equations. Following this, we report results of investigations of the different RSF laws listed above. It appeared that α was dependent on the form of the state-evolution equation and was insensitive to the frictional parameters for all laws except the PRZ law. Discussions on the underlying mechanism of $\alpha = 2$, which is representative for some state-evolution equations, implications for different loading conditions, and future study toward improvement of the friction law follows.

2. RSF laws and Voight's model

In the typical form of RSF laws, the friction coefficient or normalized shear stress by the effective normal stress f is expressed as

$$f(V, \theta) = f_* + a \ln\left(\frac{V}{V_*}\right) + b \ln\left(\frac{\theta}{\theta_*}\right), \tag{4}$$

where a and b are nondimensional parameters indicating the amount of the direct and evolution effects, respectively, and θ represents the state of the frictional surface which evolves. Note that in creep tests, both the shear and normal stresses, and thus f are kept constant. The parameters with a subscript $*$ are values at a reference state, which we can arbitrarily select as long as $f(V_*, \theta_*) = f_*$ agrees with the property of the modeled shear zone. Alternatively, f can be expressed as

$$f = a \ln\left(\frac{V}{V_*}\right) + \Theta, \tag{5}$$

where Θ is referred to as frictional strength, which is the instantaneous normalized shear stress required to slip the shear zone at the reference slip rate V_* (Nakatani, 2001). The definition of the strength depends on the selection of V_* because the RSF law generally yields a mathematically non-zero slip rate and the "stop"

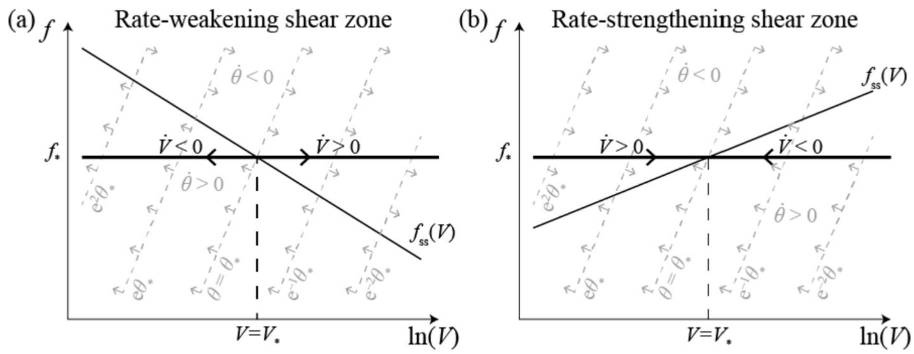

Fig. 2. Behavior of RSF shear zones under a constant f. (a) Rate-weakening shear zones, and (b) rate-strengthening shear zones. Thin black lines indicate a steady-state friction coefficient $f_{ss}(V)$, and gray dashed lines are contours of the constant θ, representing instantaneous response of the shear zones with a change in f. Gray arrows indicate the direction of the state evolution. Horizontal thick black lines and related arrows show trajectories during creep tests.

state cannot be naturally defined. The logarithmic functions in Eq. (4) are sometimes regularized either by using a $\sinh^{-1}$ function (Rice et al., 2001) or adding 1 to their arguments (Shibazaki and Shimamoto, 2007) based on considerations of elementary processes and the avoidance of divergence at $V = 0$. More than 1 state variable may be required to fit an RSF law to experimental results (e.g., Blanpied et al., 1998). In experiments for a logarithmically wide range of V values, the frictional parameters often show dependency on V (e.g., Dieterich, 1978), which can be implemented by writing expressing a and b as functions of V and θ, respectively (Noda et al., 2017). Despite these complexities, we will use Eq. (4) in this study for simplicity. a is always positive (Rice et al., 2001), and b is typically positive in the brittle regime. A negative value of b occurs in the plastic and transitional regimes and for clayey material in the term for the second state variable (e.g., Blanpied et al., 1998; Noda and Shimamoto, 2009, 2010). The focus of this study is the acceleration associated with a rate-weakening shear zone and therefore it is assumed that $b > 0$.

The state-evolution equation expresses the time derivative of θ in terms of V and θ (Ruina, 1983),

$$\dot{\theta} = g(V, \theta; L), \tag{6}$$

where L is the characteristic slip displacement of the state evolution. Existence of the steady state is usually postulated;

$$g(V, \theta_{ss}(V); L) = 0, \tag{7}$$

$$f_{ss}(V) = f(V, \theta_{ss}(V)). \tag{8}$$

The value of f approaches $f_{ss}(V)$ when V is fixed. Positive and negative $\mathrm{d}f_{ss}/\mathrm{d}\ln(V)$ correspond to rate-strengthening and rate-weakening shear zones, respectively. As mentioned in Introduction, various functional forms of g have been proposed. We discuss and analyze consequence of each formula of g.

This study mainly considers the behavior of the shear zone under a constant stress state. This condition is artificially realized in the creep test and may be applicable to the acceleration of some landslides. The effect of temporal changes in the loading condition is discussed in later sections. We selected the constant normalized shear stress as f_* and the corresponding steady-state slip rate as V_*. Usually, V_* is first chosen arbitrarily, and then f_* is set as $f_{ss}(V_*)$. In this way, f during a creep test, in general, differs from f_*, and the mathematics presented in the present study becomes involved by much. The choice of f_* adopted here causes no loss of generality and makes equations simpler. Therefore,

$$f_* = f_{ss}(V_*), \theta_* = \theta_{ss}(V_*). \tag{9}$$

Helmstetter et al. (2004) classified the behavior in the creep test into 4 cases, as combinations of rate weakening or rate strengthening and acceleration or deceleration (Fig. 2). Since θ positively correlates with frictional strength, $\dot{\theta}$ has the opposite sign to $f - f_{ss}(V)$ (Fig. 3 in Ruina, 1983). As f is constrained at f_*, the steady-state solution $V = V_*$ is unstable for a rate-weakening shear zone (Fig. 2a) and stable for a rate-strengthening shear zone (Fig. 2b). The acceleration for a rate-strengthening shear zone approaches zero as V approaches V_*. The tertiary creep behavior and the acceleration of a landslide leading to catastrophic failure correspond to the acceleration for a rate-weakening fault. Note that the simple RSFs investigated here cannot produce non-monotonic evolution in V under constant f. Therefore, structural evolution during a creep test is a key to understanding the series of primary, secondary, and tertiary creeps (Fig. 1). The focus of the present study is put on the behavior of the shear zone in the tertiary creep.

Among laboratory studies on RSF, creep tests have been only rarely conducted. Dieterich (1981) reported creep tests for granite gouge and demonstrated the transition between acceleration and deceleration depending on the applied shear stress which is kept constant. A special kind of slide-hold-slide (SHS) tests where f is kept constant during a hold period (e.g., Nakatani and Mochizuki, 1996; Nakatani, 2001) can be regarded as creep tests. However, the main purpose of the SHS tests so far was to examine the strengthening of the fault during a hold period so that f_* was smaller than f_{ss} in the preceding slide period. Then slip necessarily decelerates during the hold period (Fig. 2a). The tertiary creep is expected after an increment in f from f_{ss}. Note that conventional SHS tests that realize a hold period by halting the actuator cannot constitute a creep test because f during a hold period keeps decreasing as the continuing slow slip of the sample causes elastic relaxation of the loading system.

In the creep tests, where f is held at f_*, Eq. (4) becomes

$$v = \phi^{-\beta}, \tag{10}$$

after nondimensionalization and normalization, with v as the nondimensional slip rate V/V_*, ϕ the normalized state variable θ/θ_*, and $\beta = b/a$. Note that β is close to one in many experiments but can be as low as 0.1 or so (antigorite gouge studied by Reinen et al. (1992). Eq. (10) means v increases as the strength decreases. The state-evolution equation (Eq. (6)) is nondimensionalized to

$$\frac{\mathrm{d}\phi}{\mathrm{d}s} = \gamma(v, \phi) = \left(\frac{L}{\theta_* V_*}\right) g(V, \theta; L), \tag{11}$$

where s is nondimensional time tV_*/L. Therefore, nondimensional acceleration is expressed as

$$\frac{\mathrm{d}v}{\mathrm{d}s} = -\beta\phi^{-\beta-1}\frac{\mathrm{d}\phi}{\mathrm{d}s}. \tag{12}$$

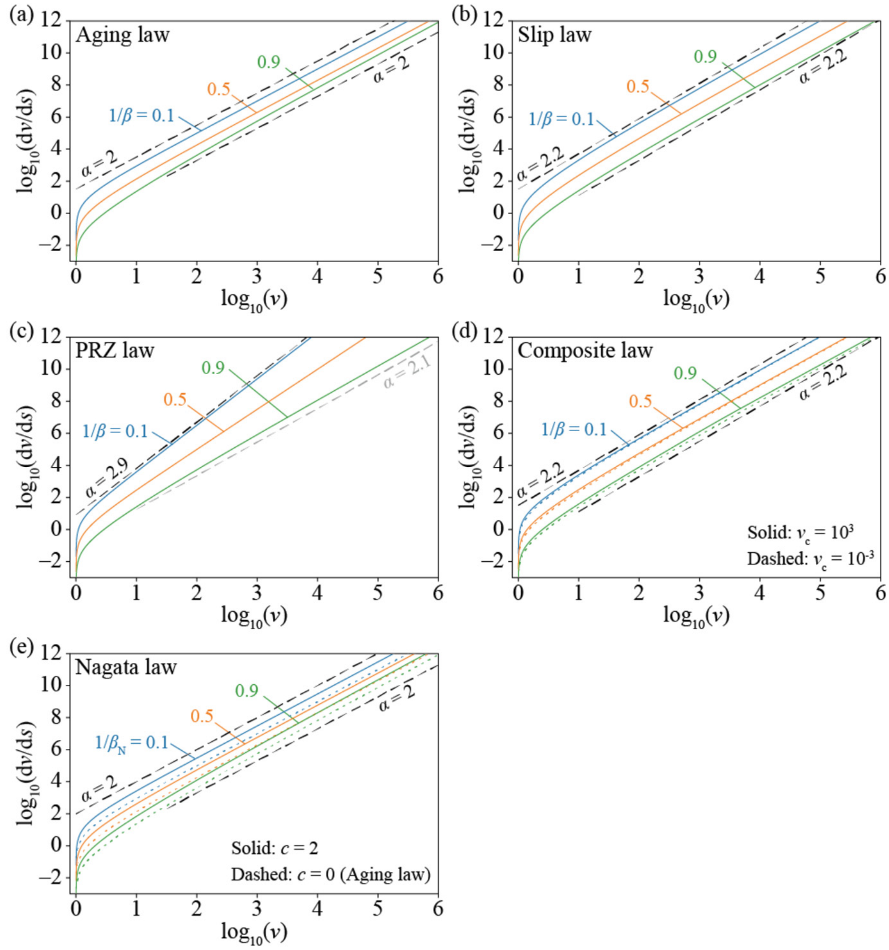

Fig. 3. Nondimensional acceleration as a function of nondimensional slip rate for various RSF laws. (a) Aging law, (b) Slip law, (c) PRZ law, (d) Composite law, and (e) Nagata law. Blue, orange, and green lines indicate (a-d) $1/\beta$ or (e) $1/\beta_N$ of 0.1, 0.5, and 0.9, respectively.

Using Eq. (11), we can denote the acceleration in terms of v as

$$\frac{dv}{ds} = -\beta v^{1+\frac{1}{\beta}} \gamma \left(v, v^{-1/\beta}\right). \tag{13}$$

A comparison of Eqs. (2) and (13) or Eq. (3) indicates that α generally depends on β and the functional form of γ. The variation of the tertiary creep behavior for different RSF laws is analyzed in the following subsections.

2.1. Aging law

Helmstetter et al. (2004) showed $\alpha = 2$ for the aging law by solving the system of equations for the slip rate as a function of time. Our Eq. (13) presents the same results. In the aging law, $\dot{\theta}$ is expressed as (Ruina, 1983)

$$g\left(V, \theta; L\right) = 1 - \frac{V\theta}{L}, \tag{14}$$

and thus

$$\theta_* = \frac{L}{V_*}, \tag{15}$$

and

$$f_{ss} = f_* + (a-b)\ln\left(\frac{V}{V_*}\right). \tag{16}$$

Ruina (1983) has shown that the state variable θ represents recent slowness; therefore, this law is also called the slowness law (Beeler et al., 1994). Nondimensionalization leads to

$$\gamma\left(v, \phi\right) = 1 - v\phi, \tag{17}$$

and Eq. (13) becomes

$$\frac{dv}{ds} = \beta v^2 \left(1 - v^{-\frac{\beta-1}{\beta}}\right). \tag{18}$$

The aging law is rate-weakening if $\beta > 1$. In this case, $dv/ds > 0$ for $v > 1$. The acceleration is approximated as $dv/ds \approx \beta v^2$ at $v \gg 1$, and thus $\alpha \approx 2$ regardless of β as shown in Fig. 3a. A in Voight's model is expected to be proportional to β. Evaluation of α (Eq. (3)) results in

$$\alpha = 2 + \frac{\beta - 1}{\beta} v^{-\frac{\beta-1}{\beta}} \left(1 - v^{-\frac{\beta-1}{\beta}}\right)^{-1}. \tag{19}$$

Here, α is larger than 2, and it decays following a power law in terms of v because $\beta > 1$.

2.2. Slip law

In the slip raw (Ruina, 1983), $\dot{\theta}$ is expressed as

$$g\left(V, \theta; L\right) = -\frac{V\theta}{L}\ln\left(\frac{V\theta}{L}\right). \tag{20}$$

Therefore, Eqs. (15) and (16) hold similarly to the aging law. Nondimensionalization leads to

$$\gamma\left(v, \phi\right) = -v\phi \ln\left(v\phi\right), \tag{21}$$

and Eq. (13) becomes

$$\frac{\mathrm{d}v}{\mathrm{d}s} = (\beta - 1)\, v^2 \ln(v)\,. \tag{22}$$

In a rate-weakening case ($\beta > 1$), acceleration is positive if $v > 1$. Fig. 3b indicates that $\alpha \approx 2.2$ if $1 < v < 10^6$. Comparison with Eq. (2) suggests that A is proportional to $\beta - 1$. Eq. (3) yields

$$\alpha = 2 + \frac{1}{\ln(v)}. \tag{23}$$

Here, α is larger than 2, and it decays slowly ($\sim 1/\ln(v)$) as v increases.

2.3. PRZ law

In the Perrin-Rice-Zheng (PRZ) law (Perrin et al., 1995), $\dot{\theta}$ is expressed as

$$g(V, \theta; L) = 1 - \left(\frac{V\theta}{2L}\right)^2. \tag{24}$$

The steady-state value of θ at $V = V_*$ is

$$\theta_* = \frac{2L}{V_*}. \tag{25}$$

The steady-state value of θ differs from Eq. (15) by a constant factor, and Eq. (16) holds. Nondimensionalization and normalization lead to

$$\gamma(v, \phi) = \frac{1}{2}\left(1 - v^2\phi^2\right), \tag{26}$$

and Eq. (13) becomes

$$\frac{\mathrm{d}v}{\mathrm{d}s} = \frac{\beta}{2} v^{3-\frac{1}{\beta}} \left(1 - v^{-2\frac{\beta-1}{\beta}}\right). \tag{27}$$

In a rate-weakening case ($\beta > 1$), acceleration is positive if $v > 1$. A comparison with Eq. (2) indicates that $\alpha \approx 3 - 1/\beta > 2$ at $v \gg 1$ as shown in Fig. 3c, and A is proportional to β. Eq. (3) yields

$$\alpha = \left(3 - \frac{1}{\beta}\right) + 2\frac{\beta - 1}{\beta} v^{-2\left(\frac{\beta-1}{\beta}\right)} \left(1 - v^{-2\left(\frac{\beta-1}{\beta}\right)}\right)^{-1}. \tag{28}$$

Here, α is larger than $3 - 1/\beta$, and it decays following a power law in terms of v; α at a large v depends on β in the PRZ law.

2.4. Composite law

In the composite law (Kato and Tullis, 2001), $\dot{\theta}$ is expressed as

$$g(V, \theta; L) = \exp\left(-\frac{V}{V_c}\right) - \frac{V\theta}{L} \ln\left(\frac{V\theta}{L}\right), \tag{29}$$

where V_c is the cut-off slip rate of log-t healing. The steady-state value of θ at $V = V_*$ is

$$\theta_* = \frac{L}{V_*} \exp\left(W\left(\exp\left(-\frac{V_*}{V_c}\right)\right)\right), \tag{30}$$

where W is the Lambert Omega function. f_{ss} is expressed as

$$f_{ss} = f_* + (a - b)\ln\left(\frac{V}{V_*}\right) + b\left[W\left(\exp(-\xi)\right)\right]_{\xi = V_*/V_c}^{\xi = V/V_c}. \tag{31}$$

Note that $\mathrm{d}f_{ss}/\mathrm{d}\ln(V)$ significantly differs from $a - b$ near $V = V_c$ (Fig. 5 and 6 in Kato and Tullis, 2001). We are interested in runaway behavior of a landslide; therefore, we assume $a - b < 0$ ($\beta > 1$), whereby f_{ss} becomes a monotonically decreasing function of V. Nondimensionalization and normalization lead to

$$\gamma(v, \phi) = \exp(-W_c)\exp\left(-\frac{v}{v_c}\right) - v\phi\left[\ln(v\phi) + W_c\right], \tag{32}$$

where $v_c = V_c/V_*$ and $W_c = W(\exp(-1/v_c))$. If $V_c \ll V_* < V$, then $W_c \approx 0$ and $v/v_c \gg 1$. In this limit, Eq. (32) becomes identical to the nondimensionalized state-evolution equation for the slip law (Eq. (21)). Using Eq. (32) in Eq. (13), we obtain

$$\frac{\mathrm{d}v}{\mathrm{d}s} = (\beta - 1)\, v^2 \ln(v) + \beta v^2 W_c - \beta \exp(-W_c)\, v^{1+\frac{1}{\beta}} \times \exp\left(-\frac{v}{v_c}\right). \tag{33}$$

The leading term is $(\beta - 1)\, v^2 \ln(v)$, which is identical to $\mathrm{d}v/\mathrm{d}s$ for the slip law (Eq. (22)). Fig. 3d shows $\mathrm{d}v/\mathrm{d}s$ for small (10^{-3}) and large (10^3) values of v_c. The case with $v_c = 10^{-3}$ is indistinguishable from that with the slip law, and v_c affects the acceleration behavior only modestly.

2.5. Nagata law

Nagata et al. (2012) proposed a friction law based on monitoring of the transmissivity of a high-frequency elastic wave across a frictional interface, which correlates with frictional strength. Nagata law reads as

$$f = a_N \ln\left(\frac{V}{V_*}\right) + \Theta_N, \tag{34}$$

$$\frac{\mathrm{d}\Theta_N}{\mathrm{d}t} = \frac{b_N V_*}{L_N} \exp\left(-\frac{\Theta_N - f_*}{b_N}\right) - \frac{b_N V}{L_N} - c\frac{\mathrm{d}f}{\mathrm{d}t}. \tag{35}$$

Here, a_N is the increase in f with an e-fold increase in V under a fixed Θ_N, $a_N - b_N$ is $\partial f_{ss}/\partial \ln(V)$, L_N is a length scale of the state evolution, and c represents the amount of the reduction of Θ_N due to shear stress change. Nagata et al. (2012) reported an optimum value of c of 2 in their rock-on-rock friction experiments for granite. This law is identical to the aging law if $c = 0$. It should be noted that if θ_N is defined in the same manner with Eqs. (4) and (5),

$$\Theta_N = f_* + b_N \ln\left(\frac{\theta_N}{\theta_{N*}}\right), \tag{36}$$

then the time derivative of θ_N cannot be expressed as a function only of V and θ_N. This is the reason for adding subscripts $_N$ to the values for Eqs. (34) and (35) to distinguish them from those of Eqs. (4) and (6).

If we redefine a state variable as

$$\theta = \exp\left(\frac{\Theta_N - f_* + ca\ln(V/V_*)}{b}\right), \tag{37}$$

then Nagata law can be expressed by Eq. (4) and

$$g(V, \theta; L) = \frac{V}{L}\left[\left(\frac{V}{V_*}\right)^{\frac{ca}{b}-1} - \theta\right], \tag{38}$$

where

$$a = \frac{a_N}{1 + c}, \quad b = b_N, \quad \text{and} \quad L = (1 + c)\, L_N. \tag{39}$$

θ defined by Eq. (37) is nondimensional, while it has the dimension of time in the other RSFs studied in the present study. The apparent amount of the direct effect a is smaller than a_N by a factor of $1 + c$ as reported by Nagata et al. (2012). Also, the larger L than L_N by a factor of $1 + c$ can be anticipated from the expression of critical stiffness derived by Kame et al. (2013). A rate-weakening shear zone corresponds to a $\beta_N = b_N/a_N > 1$ and thus $\beta > 1 + c$.

Eq. (38) matches what Ruina (1983) proposed as an example of the state variable representing a recent slip rate to a power different from -1. The steady-state value of θ at $V = V_*$ is

$$\theta_* = 1. \tag{40}$$

Nondimensionalization leads to

$$\gamma(v, \phi) = v^{\frac{c}{\beta}} - v\phi, \tag{41}$$

and the nondimensionalized acceleration (Eq. (13)) becomes

$$\frac{dv}{ds} = \beta v^2 \left(1 - v^{-\frac{\beta-(1+c)}{\beta}}\right), \tag{42}$$

which is similar to that for the aging law (Eq. (18)). The value of α is approximately 2 regardless of β (Fig. 3e), and A is expected to be proportional to $\beta = (1+c)\,\beta_N$. α is expressed as (Eq. (3))

$$\alpha = 2 + \frac{\beta-(1+c)}{\beta} v^{-\frac{\beta-(1+c)}{\beta}} \left(1 - v^{-\frac{\beta-(1+c)}{\beta}}\right)^{-1}. \tag{43}$$

Here, α is larger than 2, and it decays following a power law in terms of v.

3. Discussion

3.1. Limitation of the present model

In this study, behavior of a shear zone governed by various RSF laws was investigated under a constant stress state. This is a highly idealized system with only one degree of freedom, while the behavior of real landslides is more complex and thus applicability of the present model should be considered. For example, landslides can spread laterally with overall extensions (e.g., Varnes, 1978). In such a landslide, the slip on the underlying shear zone is not uniform so that a system with only one degree of freedom may be insufficient. In addition, internal inelastic deformation of the landslide may contribute significantly to Ω. If this is the case, observed behavior should be compared with a model of flow of the landslide mass so that the present model is not applicable. Even if the landslide does not spread, rupture propagation along the shear zone may occur in the preparation process (e.g., Cooper et al., 1998; Petley et al., 2002, 2005). In this case, the present model is applicable when the rupture has spanned the entire shear zone and block motion relative to the footwall becomes dominant. Even before this point, acceleration of the surface displacement may occur due to quasistatic crack growth, but its interpretation using the present model would lead to significant error. Quasistatic rupture propagation and concurrent slip acceleration have been studied in the context of earthquake nucleation process and were shown to depend on the form of the RSF law (e.g., Ampuero and Rubin, 2008). Investigation of the dynamics of heterogeneous slip evolution (e.g., Handwerger et al., 2016) and comparison of different RSF laws in system settings that are more relevant to the landslide preparation process deserve future study.

We investigated several RSF laws, and found that α was consistently larger than 2, and decayed to 2 with increasing v except for under the PRZ law. A typical α from observations of real landslides approximates 2 (e.g., Segalini et al., 2018), but can be significantly smaller (Bozzano et al., 2014). The list of the studied laws is incomplete, as there are more recently proposed friction laws (e.g., Chen and Spiers, 2016; Li and Rubin, 2017). Investigation of those friction laws in terms of the tertiary creep test may be important. It is likely that different mechanisms from those studied here are dominant in landslides with significantly smaller α values than 2, such as the change in the stress state including pore pressure (e.g., Terzaghi, 1950; Hendron and Patton, 1985; Leroueil, 2001), different weakening mechanisms such as pore pressure generation by compaction (e.g., Iverson et al., 2000) and hydrothermal effects due to frictional heating (e.g., Veveakis et al., 2007). These effects on behavior of a shear zone governed by the RSF laws are discussed in following subsections.

Another possible factor that was not investigated in the present study but may cause a smaller α is the development and structural evolution of the shear zone and associated change in frictional properties. RSF laws are established based on friction experiments at a sufficiently long slip displacement for the steady-state friction to be recognized. Therefore, structural evolution with less shear strain is not considered. Rotary-shear friction experiments capable of producing infinitely long slip displacements (Beeler et al., 1996) revealed that structural evolution causes the change in the rate dependency in a complex manner. Frictional properties of the shear zone under structural evolution deserve future study.

3.2. $\alpha = 2$ for linearly slip-dependent $f - \Theta$

Among the RSF laws studied, α decayed to 2 rapidly as v increased for the aging law and Nagata law. These laws are known to cause nearly linear slip weakening, in the context of RSF, on a positive velocity step by a factor larger than approximately 100 (Nakatani, 2001; Ampuero and Rubin, 2008; Bhattacharya and Rubin, 2014). If $v\phi \gg 1$ in the aging law or if $v\phi \gg v^{c/\beta}$ in Nagata law, the first term in the right-hand side of Eqs. (17) and (41) is negligible and thus

$$\frac{d\phi}{d\delta} \approx -\phi, \tag{44}$$

where δ is nondimensional slip given by $d\delta = v ds$. ϕ and Θ are then approximated as

$$\phi \approx \phi_0 \exp(-\delta), \quad \text{and} \quad \Theta \approx f_* + b\ln(\phi_0) - b\delta = \Theta_0 - b\delta, \tag{45}$$

where the subscript $_0$ indicates the initial value. The frictional strength Θ decreases almost linearly with the slip, independent of the slip rate when $v\phi$ is large. From Eq. (5), the slip rate and acceleration are expressed as

$$v = \exp\left(\frac{f-\Theta}{a}\right), \quad \text{and} \quad \frac{dv}{ds} = \left(\frac{df}{ds} - \frac{d\Theta}{ds}\right)\frac{v}{a}. \tag{46}$$

Eq. (45) leads to

$$\frac{dv}{ds} = \left(\frac{1}{a}\frac{df}{ds} + \beta v\right) v. \tag{47}$$

This results in the leading term of Eqs. (18) and (42) when f is constant. This analysis shows that $\alpha = 2$ may be a consequence of the rate-independent linear slip weakening and a logarithmic direct effect. The existence of steady state is no longer relevant.

A similar discussion to this can be made to bulk deformation. Brantut et al. (2014) compared a triaxial deformation test at a constant strain rate and a creep test at a constant load, and proposed a rate- and strain-dependent constitutive law for a brittle failure. The differential stress during a creep test σ_d^{cr} is expressed as (Eq. (2) in Brantut et al. (2014))

$$\sigma_d^{cr} = \sigma_* \ln\left(\frac{\dot{\epsilon}^{cr}}{\dot{\epsilon}^{str}}\right) + \sigma_d^{str}\left(\epsilon^{cr}\right), \tag{48}$$

where ϵ^{cr} and $\dot{\epsilon}^{cr}$ are the strain during the creep test and the strain rate, respectively, σ_d^{str} is the differential stress at a constant strain rate ($\dot{\epsilon}^{str}$), and σ_* is the characteristic activation stress. σ_d^{str} is a function of strain, and presents strength in the same manner as Θ in Eq. (5). Solving for $\dot{\epsilon}^{\mathrm{cr}}$ and taking a derivative with respect to time, we obtain

$$\ddot{\epsilon}^{\mathrm{cr}} = -\frac{\sigma_{\mathrm{d}}^{\mathrm{str}'}\left(\epsilon^{cr}\right)}{\sigma_*}\dot{\epsilon}^{\mathrm{cr}2}, \tag{49}$$

if the applied stress $\sigma_{\mathrm{d}}^{\mathrm{cr}}$ is constant. This infers that $\alpha = 2$ if $\sigma_{\mathrm{d}}^{\mathrm{str}}$ is a decreasing function of strain and its derivative does not change significantly.

Eq. (46) indicates that the difference between f and Θ is relevant. Therefore, $\alpha = 2$ is also recovered if the increase in f dominates over the change in Θ and can be approximated as a linear function of slip independently of the slip rate. For example, shear-induced compaction (e.g., Iverson et al., 2000) or frictional heating (e.g., Veveakis et al., 2007) builds up pore fluid pressure, decreasing the effective normal stress and increasing f. If the deformation becomes so rapid that transports of fluid and heat are neglected, then f can be expressed as a function of the slip. These mechanisms can cause runaway behavior of a landslide even if the shear zone is rate strengthening.

3.3. Time-dependent weakening decreases $\boldsymbol{\alpha}$

It has been shown that $\alpha = 2$ corresponds to the linear increase in $f - \Theta$ with slip independent of the slip rate. The other extreme situation may be purely time-dependent weakening or loading. If linearization is a good approximation, $\mathrm{d}\Theta/\mathrm{d}s$ or $\mathrm{d}f/\mathrm{d}s$ can be regarded constant and thus Eq. (46) suggests $\alpha = 1$. Although typical observation of $\alpha = 2$ negates the dominance of the time-dependent effect in actual landslides, we would like to point out that a combination of the slip-dependent and time-dependent effects may cause values of α between 1 and 2. Eq. (47) suggests that $\alpha \approx 1$ if $v \ll \mathrm{d}f/b\mathrm{d}s$, and it increases with acceleration, and $\alpha \approx 2$ if $v \gg \mathrm{d}f/b\mathrm{d}s$. The observation of $\alpha < 1$ (Bozzano et al., 2014) cannot be explained by the introduction of time-dependent loading or weakening. Modification of the direct effect from the logarithmic function to, for example, a power law (e.g., Noda and Shimamoto (2010) for ductile deformation of NaCl) or implementation of a change in the frictional properties associated with structural evolution of the shear zone may be required.

3.4. Future study in refining the RSF law

In investigations of the RSF law using laboratory experiments, the velocity-step test and the SHS test are commonly used (e.g., Marone, 1998; Bhattacharya et al., 2022), while tertiary creep tests (Dieterich, 1981) have been rarely conducted. Creep tests under deceleration condition have been conducted in SHS tests during the hold periods (e.g., Nakatani and Mochizuki, 1996; Nakatani, 2001; Nagata et al., 2008). The main application of the RSF law has been with regard to modeling of earthquake generation processes (e.g., Lapusta et al., 2000). For earthquakes, acceleration of slow slip to seismic slip rate has been rarely observed, and tertiary creep tests do not have their counterpart observations for direct comparison. Nevertheless, tertiary creep tests are likely useful in constraining the state-evolution equation through the Voight model and Eq. (13). Tertiary creep tests for rocks and fault gouges would provide new insights into the form of the RSF law.

4. Conclusion

Acceleration of a landslide toward catastrophic failure follows the Voight power-law model with the power exponent α, which is typically close to 2 but can be significantly smaller. A previous study (Helmstetter et al., 2004) showed that $\alpha = 2$ is realized in a behavior of a shear zone under constant f (= shear stress / effective normal stress) governed by the RSF law in the form of the aging law. The present study extended the analyses of the creep behavior to different forms of the RSF laws. In addition to the aging law, the slip, PRZ, composite, and Nagata laws were investigated as representative examples. Acceleration was expressed in terms of the slip rate using the state-evolution equation. For the aging and Nagata laws, α decays to 2 following a power law in terms of the nondimensional slip rate v. For the slip and composite laws, α decays to 2 slowly in a manner of $1/\ln(v)$, while for the PRZ law, α decays to $3 - a/b$ where a and b are frictional parameters in the RSF law.

The aging and Nagata laws are characterized by an almost linear slip weakening after a positive velocity step of a large factor. The weakening per slip increment is independent of the slip rate. It was shown that the combination of the logarithmic direct effect and the linear rate-independent slip-weakening or slip-dependent increase in f results in $\alpha = 2$. In the other end-member case, a purely time-dependent weakening and, equivalently, a change in f with time lead to $\alpha = 1$. Explanations of smaller values of α may require a different rate dependency from the standard logarithmic direct effect.

Tertiary creep tests have been rarely conducted in laboratory rock-friction experiments for investigation of the RSF laws. They could provide new insights on the form of the state-evolution equation through the Voight model and thus deserve future study.

Studies in humans and animals

The present study does not involve any human subject or animal experiment.

Funding

The present study was supported by the Ministry of Education, Culture, Sports, Science and Technology (MEXT) of Japan under its Second Earthquake and Volcano Hazards Observation and Research Program (Earthquake and Volcano Hazard Reduction Research) and by JSPS KAKENHI Grant Number 21H05201.

CRediT authorship contribution statement

Hiroyuki Noda: Conceptualization, Formal analysis, Funding acquisition, Investigation, Methodology, Software, Visualization, Writing – original draft, Writing – review & editing. **Chengrui Chang:** Conceptualization, Writing – original draft, Writing – review & editing.

Declaration of competing interest

The authors declare that they have no known competing financial interests or personal relationships that could have appeared to influence the work reported in this paper.

Data availability

No data was used for the research described in the article.

Acknowledgements

The authors thank T. Yamaguchi for discussion. The comments by the editor and 2 reviewers were very useful in improving the manuscript.

References

Ampuero, J.-P., Rubin, A.M., 2008. Earthquake nucleation on rate and state faults – aging and slip laws. J. Geophys. Res., Solid Earth 113, B01302. https://doi.org/10.1029/2007JB005082.

Beeler, N.M., Tullis, T.E., Weeks, J.D., 1994. The roles of time and displacement in the evolution effect in rock friction. Geophys. Res. Lett. 21, 1987–1990. https://doi.org/10.1029/94GL01599.

Beeler, N.M., Tullis, T.E., Blanpied, M.L., Weeks, J.D., 1996. Frictional behavior of large displacement experimental faults. J. Geophys. Res., Solid Earth 101, 8697–8715. https://doi.org/10.1029/96JB00411.

Bhattacharya, P., Rubin, A.M., 2014. Frictional response to velocity steps and 1-D fault nucleation under a state evolution law with stressing-rate dependence. J. Geophys. Res., Solid Earth 119, 2272–2304. https://doi.org/10.1002/2013JB010671.

Bhattacharya, P., Rubin, A.M., Bayart, E., Savage, H.M., Marone, C., 2015. Critical evaluation of state evolution laws in rate and state friction: fitting large velocity steps in simulated fault gouge with time-, slip-, and stress-dependent constitutive laws. J. Geophys. Res., Solid Earth 120, 6365–6385. https://doi.org/10.1002/2013JB010671.

Bhattacharya, P., Rubin, A.M., Beeler, N.M., 2017. Does fault strengthening in laboratory rock friction experiments really depend primarily upon time and not slip? J. Geophys. Res., Solid Earth 122, 6389–6430. https://doi.org/10.1002/2017JB013936.

Bhattacharya, P., Rubin, A.M., Tullis, T.E., Beeler, N.M., Okazaki, K., 2022. The evolution of rock friction is more sensitive to slip than elapsed time, even at near-zero slip rates. Proc. Natl. Acad. Sci. 119, e2119462119. https://doi.org/10.1073/pnas.2119462119.

Blanpied, M.L., Marone, C.J., Lockner, D.A., Byerlee, J.D., King, D.P., 1998. Quantitative measure of the variation in fault rheology due to fluid-rock interactions. J. Geophys. Res., Solid Earth 103, 9691–9712. https://doi.org/10.1029/98JB00162.

Bozzano, F., Cipriani, I., Mazzanti, P., Prestininzi, A., 2014. A field experiment for calibrating landslide time-of-failure prediction functions. Int. J. Rock Mech. Min. Sci. 67, 69–77. https://doi.org/10.1016/j.ijrmms.2013.12.006.

Brantut, N., Heap, M.J., Baud, P., Meredith, P.G., 2014. Rate- and strain-dependent brittle deformation of rocks. J. Geophys. Res., Solid Earth 119, 1818–1836. https://doi.org/10.1002/2013JB010448.

Chen, J., Spiers, C.J., 2016. Rate and state frictional and healing behavior of carbonate fault gouge explained using microphysical model. J. Geophys. Res., Solid Earth 121, 8642–8665. https://doi.org/10.1002/2016JB013470.

Cooper, M.R., Bromhead, E.N., Petley, D.J., Grants, D.I., 1998. The Selborne cutting stability experiment. Géotechnique 48, 83–101. https://doi.org/10.1680/geot.1998.48.1.83.

Crosta, G.B., Agliardi, F., 2003. Failure forecast for large rock slides by surface displacement measurements. Can. Geotech. J. 40, 176–191. https://doi.org/10.1139/t02-085.

Dieterich, J.H., 1972. Time-dependent friction in rocks. J. Geophys. Res. 77, 3690–3697. https://doi.org/10.1029/JB077i020p03690.

Dieterich, J.H., 1978. Time-dependent friction and the mechanics of stick-slip. Pure Appl. Geophys. 116, 790–806. https://doi.org/10.1007/BF00876539.

Dieterich, J.H., 1979. Modeling of rock friction: 1. Experimental results and constitutive equations. J. Geophys. Res., Solid Earth 84, 2161–2168. https://doi.org/10.1029/JB084iB05p02161.

Dieterich, J.H., 1981. Constitutive properties of faults with simulated gouge. In: Mechanical Behavior of Crustal Rocks. American Geophysical Union (AGU), pp. 103–120.

Dieterich, J.H., Kilgore, B.D., 1994. Direct observation of frictional contacts: new insights for state-dependent properties. Pure Appl. Geophys. 143, 283–302. https://doi.org/10.1007/BF00874332.

Federico, A., Popescu, M., Elia, G., Fidelibus, C., Internò, G., Murianni, A., 2012. Prediction of time to slope failure: a general framework. Environ. Earth Sci. 66, 245–256. https://doi.org/10.1007/s12665-011-1231-5.

Fukuzono, T., 1985. A new method for predicting the failure time of a slope. In: Proceedings of 4th International Conference and Field Workshop on Landslide. 1985, pp. 145–150.

Handwerger, A.L., Rempel, A.W., Skarbek, R.M., Roering, J.J., Hilley, G.E., 2016. Rate-weakening friction characterizes both slow sliding and catastrophic failure of landslides. Proc. Natl. Acad. Sci. 113, 10281–10286. https://doi.org/10.1073/pnas.1607009113.

Helmstetter, A., Sornette, D., Grasso, J.-R., Andersen, J.V., Gluzman, S., Pisarenko, V., 2004. Slider block friction model for landslides: application to Vaiont and La Clapière landslides. J. Geophys. Res., Solid Earth 109. https://doi.org/10.1029/2002JB002160.

Hendron Jr., A.J., Patton, F.D., 1985. The Vaiont Slide, a Geotechnical Analysis Based on New Geologic Observations of the Failure Surface. Volume I Main Text (Technical Report No. GL-85-5). U.S. Army Engineer Waterways Experiment, Vicksburg, MS.

Intrieri, E., Raspini, F., Fumagalli, A., Lu, P., Del Conte, S., Farina, P., Allievi, J., Ferretti, A., Casagli, N., 2018. The Maoxian landslide as seen from space: detecting precursors of failure with Sentinel-1 data. Landslides 15, 123–133. https://doi.org/10.1007/s10346-017-0915-7.

Intrieri, E., Carlà, T., Gigli, G., 2019. Forecasting the time of failure of landslides at slope-scale: a literature review. Earth-Sci. Rev. 193, 333–349. https://doi.org/10.1016/j.earscirev.2019.03.019.

Iverson, R.M., Reid, M.E., Iverson, N.R., LaHusen, R.G., Logan, M., Mann, J.E., Brien, D.L., 2000. Acute sensitivity of landslide rates to initial soil porosity. Science 290, 513–516. https://doi.org/10.1126/science.290.5491.513.

Kame, N., Fujita, S., Nakatani, M., Kusakabe, T., 2013. Earthquake cycle simulation with a revised rate- and state-dependent friction law. Tectonophysics 600, 196–204. https://doi.org/10.1016/j.tecto.2012.11.029.

Kato, N., Tullis, T.E., 2001. A composite rate- and state-dependent law for rock friction. Geophys. Res. Lett. 28, 1103–1106. https://doi.org/10.1029/2000GL012060.

Lacroix, P., Handwerger, A.L., Bièvre, G., 2020. Life and death of slow-moving landslides. Nat. Rev. Earth Environ. 1, 404–419. https://doi.org/10.1038/s43017-020-0072-8.

Lapusta, N., Rice, J.R., Ben-Zion, Y., Zheng, G., 2000. Elastodynamic analysis for slow tectonic loading with spontaneous rupture episodes on faults with rate- and state-dependent friction. J. Geophys. Res., Solid Earth 105, 23765–23789. https://doi.org/10.1029/2000JB900250.

Leroueil, S., 2001. Natural slopes and cuts: movement and failure mechanisms. Géotechnique 51, 197–243. https://doi.org/10.1680/geot.2001.51.3.197.

Li, T., Rubin, A.M., 2017. A microscopic model of rate and state friction evolution. J. Geophys. Res., Solid Earth 122, 6431–6453. https://doi.org/10.1002/2017JB013970.

Loew, S., Gschwind, S., Gischig, V., Keller-Signer, A., Valenti, G., 2017. Monitoring and early warning of the 2012 Preonzo catastrophic rockslope failure. Landslides 14, 141–154. https://doi.org/10.1007/s10346-016-0701-y.

Marone, C., 1998. Laboratory-derived friction laws and their application to seismic faulting. Annu. Rev. Earth Planet. Sci. 26, 643–696. https://doi.org/10.1146/annurev.earth.26.1.643.

Müller, L., 1964. The rock slide in the Vaiont Valley. Rock Mech. Eng. Geol. 2, 148–212.

Nagata, K., Nakatani, M., Yoshida, S., 2008. Monitoring frictional strength with acoustic wave transmission. Geophys. Res. Lett. 35. https://doi.org/10.1029/2007GL033146.

Nagata, K., Nakatani, M., Yoshida, S., 2012. A revised rate- and state-dependent friction law obtained by constraining constitutive and evolution laws separately with laboratory data. J. Geophys. Res., Solid Earth 117. https://doi.org/10.1029/2011JB008818.

Nakatani, M., Mochizuki, H., 1996. Effects of shear stress applied to surfaces in stationary contact on rock friction. Geophys. Res. Lett. 23, 869–872. https://doi.org/10.1029/96GL00726.

Nakatani, M., 2001. Conceptual and physical clarification of rate and state friction: frictional sliding as a thermally activated rheology. J. Geophys. Res., Solid Earth 106, 13347–13380. https://doi.org/10.1029/2000JB900453.

Noda, H., Shimamoto, T., 2009. Constitutive properties of clayey fault gouge from the Hanaore fault zone, southwest Japan. J. Geophys. Res., Solid Earth 114. https://doi.org/10.1029/2008JB005683.

Noda, H., Shimamoto, T., 2010. A rate- and state-dependent ductile flow law of polycrystalline halite under large shear strain and implications for transition to brittle deformation. Geophys. Res. Lett. 37. https://doi.org/10.1029/2010GL042512.

Noda, H., Sawai, M., Shibazaki, B., 2017. Earthquake sequence simulations with measured properties for JFAST core samples. Philos. Trans. R. Soc., Math. Phys. Eng. Sci. 375, 20160003. https://doi.org/10.1098/rsta.2016.0003.

Perrin, G., Rice, J.R., Zheng, G., 1995. Self-healing slip pulse on a frictional surface. J. Mech. Phys. Solids 43, 1461–1495. https://doi.org/10.1016/0022-5096(95)00036-I.

Petley, D.N., Bulmer, M.H., Murphy, W., 2002. Patterns of movement in rotational and translational landslides. Geology 30, 719–722. https://doi.org/10.1130/0091-7613(2002)030<0719:POMIRA>2.0.CO;2.

Petley, D.N., Higuchi, T., Petley, D.J., Bulmer, M.H., Carey, J., 2005. Development of progressive landslide failure in cohesive materials. Geology 33, 201–204. https://doi.org/10.1130/G21147.1.

Reinen, L.A., Tullis, T.E., Weeks, J.D., 1992. Two-mechanism model for frictional sliding of serpentinite. Geophys. Res. Lett. 19, 1535–1538. https://doi.org/10.1029/92GL01388.

Rice, J.R., Lapusta, N., Ranjith, K., 2001. Rate and state dependent friction and the stability of sliding between elastically deformable solids. In: The JW Hutchinson and JR Rice 60th Anniversary Issue. J. Mech. Phys. Solids 49, 1865–1898. https://doi.org/10.1016/S0022-5096(01)00042-4.

Ruina, A., 1983. Slip instability and state variable friction laws. J. Geophys. Res., Solid Earth 88, 10359–10370. https://doi.org/10.1029/JB088iB12p10359.

Saito, M., Uezawa, H., 1961. Failure of soil due to creep. In: 5th International Conference on Soil Mechanics and Foundation Engineering. Paris, pp. 315–318.

Segalini, A., Valletta, A., Carri, A., 2018. Landslide time-of-failure forecast and alert threshold assessment: a generalized criterion. Eng. Geol. 245, 72–80. https://doi.org/10.1016/j.enggeo.2018.08.003.

Shibazaki, B., Shimamoto, T., 2007. Modelling of short-interval silent slip events in deeper subduction interfaces considering the frictional properties at the unstable-stable transition regime. Geophys. J. Int. 171, 191–205. https://doi.org/10.1111/j.1365-246X.2007.03434.x.

Terzaghi, K., 1950. Mechanism of landslides. In: Paige, S. (Ed.), Application of Geology to Engineering Practice. Geological Society of America, pp. 83–123.

Varnes, D.J., 1978. Slope movement types and processes. Transportation Research Board Special Report 176, 11–33.

Veveakis, E., Vardoulakis, I., Di Toro, G., 2007. Thermoporomechanics of creeping landslides: the 1963 Vaiont slide, northern Italy. J. Geophys. Res., Earth Surf. 112. https://doi.org/10.1029/2006JF000702.

Voight, B., 1988. A method for prediction of volcanic eruptions. Nature 332, 125–130. https://doi.org/10.1038/332125a0.

Voight, B., 1989. A relation to describe rate-dependent material failure. Science 243, 200–203. https://doi.org/10.1126/science.243.4888.200.

Yang, S., Jiang, Y., 2010. Triaxial mechanical creep behavior of sandstone. Min. Sci. Technol. (China) 20, 339–349. https://doi.org/10.1016/S1674-5264(09)60206-4.

Zhang, Z.-Y., Chen, S.-M., Tao, L.-J., 2002. 1983 Sale Mountain landslide, Gansu Province, China. In: Evans, S.G., Degraff, J.V. (Eds.), Catastrophic Landslides. Geological Society of America, pp. 149–163.